Catalysis Today 175 (2011) 196–201

Contents lists available at ScienceDirect

Catalysis Today

journal homepage: www.elsevier.com/locate/cattod

Effect of alkali metal promoters on natural manganese ore catalysts for the complete catalytic oxidation of *o*-xylene

Yinsu Wu, Min Liu, Zichuan Ma*, Sheng tao Xing

College of Chemistry and Material Science, Hebei Normal University, Yuhua East Road 113#, Shijiazhuang 050016, China

ARTICLE INFO

Article history:
Received 10 October 2010
Received in revised form 22 February 2011
Accepted 12 April 2011
Available online 13 May 2011

Keywords:
Alkali metal
Natural manganese ore
o-Xylene
Complete catalytic oxidation

ABSTRACT

A series of alkali metal doped natural manganese ore (NMO) catalysts were prepared by an impregnation method, and tested for the complete catalytic oxidation of *o*-xylene. The effects of alkali metal on the catalytic performance and structural properties of NMO were examined. Alkali metals were found to enhance the activity of NMO in the following order: Li < Na < Rb < K, Cs. The experimental results showed that NMO-K(Cs)-0.07 could convert *o*-xylene (0.055 vol.%) into CO_2 and H_2O at 240 °C, which was 60 °C lower than that of NMO. X-ray diffraction (XRD), X-ray photoelectron spectroscopy (XPS) and Brunauer–Emmett–Teller (BET) measurements revealed that the primary component of NMO and NMO-K-0.07 were MnO_2. It was found that K_2O was highly dispersed onto the NMO surface. The addition of K_2O did not increase the BET surface area of the NMO. However, it resulted in the binding energy of the Mn 2p of NMO-K-0.07 shifted to a lower value. The results suggested that alkali metals act as electronic promoters, indicating that alkali metal doped NMO are promising catalyst candidates for the catalytic oxidation of VOCs.

1. Introduction

Complete catalytic oxidation techniques that convert an organic compound contaminant into CO_2 and H_2O are an effective way to remove volatile organic compounds (VOCs). Such techniques are advantageous in terms of their high destructive efficiency, low operating temperatures, and low NO_x emissions as compared to thermal combustion systems, especially for VOCs at low concentrations [1]. Two types of catalysts have been used, alone or in combination, for oxidizing VOCs pollutants: supported noble metals, and metal oxides or supported metal oxides. Supported noble metal catalysts with Pd and Pt have been generally preferred for the complete catalytic oxidation of VOCs [2–6]. However, these noble metals are expensive and sometimes show poor thermal stability [7–9]. Thus development of transition-metal-oxide-based catalysts for VOC oxidation has attracted significant interest. Manganese oxides, both supported and unsupported, are particularly catalytically active for VOC oxidation [10–13]. For instance, Einaga et al. [10] developed alumina supported manganese oxide catalysts for catalytic oxidation of benzene with ozone, and investigated the behavior of benzene oxidation and CO_x formation. Sambeth and co-workers [11] prepared two kinds of MnO_2 by $MnCO_3$ decomposition and oxidation of acidic $MnSO_4$ solution. The catalysts showed high activity for the complete oxidation of ethanol to CO_2 and H_2O. The supported manganese oxides are usually prepared by the solution impregnation method on various supports using manganese nitrate or acetate [10]. In the case of unsupported manganese oxides, only a limited number of investigations have been reported because of their generally low surface areas. It has been found that the addition of Ce, Cu or Zr oxides could increase the catalysts' surface area and catalytic activity [14,15]. Synthetic methods of Mn-containing metal oxides include a redox-precipitation method, a conventional precipitation method, a microemulsions method, a Sol–Gel method, and a solid state synthesis method [8,16]. Despite the catalytic activity of Mn-containing metal oxides, the complicated synthesis and purification procedures result in their high costs.

Natural manganese ore (NMO), which consists of a system of oxides with a high content of manganese oxide, has the potential to be utilized for the catalytic oxidation. Lee et al. [17] investigated NMOs in the selective catalytic oxidation of ammonia to nitrogen oxides. They found that NMO catalysts exhibited excellent catalytic activity towards these reactions.

A positive effect of alkali metal doping has been recently observed by several investigations in various systems [18–20]. Alkali metal compounds could serve as textural or electronic promoters for catalysts in various catalytic processes. For instance, He and co-workers [18] reported that alkali and alkaline earth metal dopants could promote the activity of cobalt–cerium composite oxides towards N_2O decomposition. They found that alkali metals

* Corresponding author. Tel.: +86 311 86268343; fax: +86 311 86269217.
E-mail address: ma_zichuan@163.com (Z. Ma).

0920-5861/$ – see front matter © 2011 Elsevier B.V. All rights reserved.
doi:10.1016/j.cattod.2011.04.023

improved the redox ability of active site Co^{2+} by acting as electronic promoters. Gandía et al. studied the effect of Cs^+ and Na^+ additions on the activity of Mn_2O_3 in the catalytic combustion of ketones [19]. They found that the presence of alkali metal additives to Mn_2O_3 increased the electron density of the Mn_2O_3 surface, and enhanced the electrophilic adsorption of ketone molecules, thus reducing the combustion temperature. Jirátová et al. investigated the catalytic activity of Co–Mn–Al mixed oxide modified with potassium for the total oxidation of toluene and ethanol. The acidity and basicity of the catalysts were changed with the change of potassium contents, and further increased catalyst reducibility [20].

In our previous study, we investigated the effects of CeO_2 on the structure and catalytic activities of MnO_2 for VOC complete catalytic oxidation [14]. Here, a series of alkali metal-doped NMO catalysts were prepared, and *o*-xylene, a major VOC, was chosen to test their catalytic oxidation performances. The aim of the present work was to study the influences of alkali metals on the performance of NMO in the catalytic combustion of VOCs. A significant increase of catalytic activity was found when alkali metal promoters were present. X-ray diffraction (XRD), Brunauer–Emmett–Teller (BET) surface area measurement, X-ray photoelectron spectroscopy (XPS), and hydrogen temperature-programmed reduction (H_2-TPR) were used to characterize these catalysts in order to investigate the origin of the effect of alkali dopants.

2. Experiments

2.1. Catalyst preparation

The alkali metal-doped NMO catalysts were prepared by the impregnation of NMO (from Guanxi province, China) with an aqueous solution containing an appropriate amount of alkali metal nitrates. The catalyst samples were dried at 110 °C for 12 h, and then calcined at 400 °C for 6 h in air. This catalyst was denoted as NMO-M-*x* ("M" indicates the doping alkali metal; "*x*" indicates the atomic ratio of M/Mn).

2.2. Catalyst characterization

The nitrogen adsorption–desorption isotherm was obtained at −196 °C using a Quantachrome Autosorb-1c instrument. The samples were degassed at 300 °C for 4 h. The isotherms were elaborated according to the BET method for calculating the surface area, and the average pore size was calculated using the BJH method. X-ray diffraction (XRD) analyses of the catalysts were performed in the 2θ range of 20–80° with a step size of 0.05 °/s using a D8-ADVANCE diffractometer (Germany) operated at 40 kV and 40 mA, and using a nickel-filtered Cu Kα(λ = 0·15418 nm) radiation source. X-ray photoelectron spectroscopy (XPS) data were obtained using a SHIMADZU ESCA-3400 spectrometer (Mg Kα radiation). The binding energy regions investigated were 280–300 eV (C1s), 522–542 eV (O 1s), and 630–670 eV (Mn 2p) using a C 1s line (284.8 eV) of adventitious carbon as a reference. The chemical composition of the NMO was analyzed with an energy dispersive spectrometer (EDS, EDAX PV9900).

2.3. H_2-TPR

Temperature programmed reduction (TPR) experiments were performed from room temperature up to 900 °C under a flow of 5% H_2/Ar mixture (30 mL min^{-1}) over 50 mg of catalyst at a heating rate of 10 °C min^{-1}. Prior to the TPR experiments, the catalysts were pre-treated in a 20% O_2/He mixture at 400 °C for 1 h to clean the surface of the catalysts. A mass spectrometer (Hiden HPR20) was used for on-line monitoring of the TPR effluent gas.

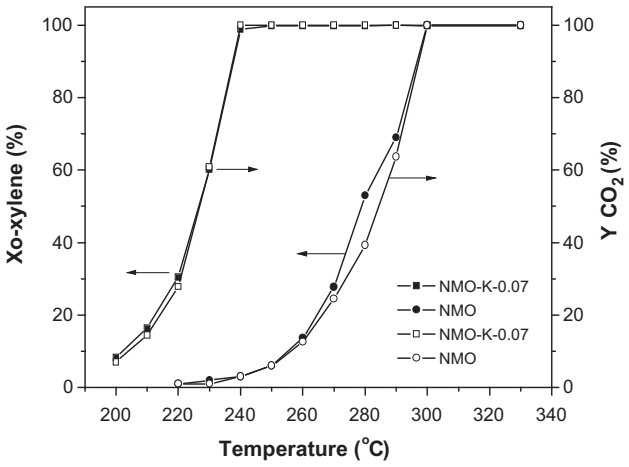

Fig. 1. *o*-Xylene conversion and CO_2 yield over the NMO and NMO-K-0.07 catalysts. Reaction conditions: *o*-xylene 550 ppm, 20% O_2/N_2 balance, total flow rate 50 mL min^{-1}, W/F = 0.60 g s mL^{-1}.

2.4. Catalytic activity measurement

Catalytic activity was measured in a 4 mm i.d. quartz tubular reactor. Approximately 0.50 g of catalyst supported by quartz wool was placed in the middle of the reactor. A gas containing 550 ppm of *o*-xylene in simulated air (20 vol.% O_2, 80 vol.% N_2) was continuously passed through the catalyst bed at a flow rate of 50 mL min^{-1} where W/F = 0.60 g s mL^{-1} (corresponding to a GHSV of 7000 h^{-1}). Here, W/F is defined as the catalyst weight divided by the gas flow rate. CO_2 was the only detectable C-containing reaction product, which initially passed through the TDX-01 stainless steel packed column, and then converted to methane in a reformer furnace; no significant concentration of any partial oxidation product was detected in the effluent. The reactant and reaction product were analyzed with an on-line gas chromatograph equipped with two flame ionization detectors (FID) in series. *o*-Xylene conversion ($X_{o\text{-xylene}}$) and the yield of CO_2 (Y_{CO2}) were calculated according to the following formulas:

$$X_{o\text{-xylene}} = \frac{(o\text{-xylene}_{in} - o\text{-xylene}_{out})}{o\text{-xylene}_{in}} \times 100 \quad (1)$$

$$Y_{CO_2} = \frac{CO_{2_{out}}/8}{o - \text{xylene}_{in}} \times 100 \quad (2)$$

3. Results and discussion

3.1. Catalytic activity measurements

3.1.1. Promoter effect of alkali metal K

Fig. 1 shows the light-off curves of *o*-xylene conversion and CO_2 yield for the NMO and the NMO-K-0.07 catalysts, respectively. Clearly, the activity of the NMO catalyst was significantly enhanced by the addition of K. The NMO-K-0.07 catalyst showed a high catalytic activity for the complete oxidation of *o*-xylene. 100% of *o*-xylene was converted into CO_2 at 240 °C, which was 60 °C lower than the required temperature for 100% *o*-xylene conversion using the NMO catalyst. Fig. 1 also shows that there was a gap between the *o*-xylene conversion and CO_2 yield at a lower temperature over the NMO catalyst. While, the *o*-xylene conversion and CO_2 yield were almost the same at all temperatures over the NMO-K-0.07 catalyst. These results indicate that alkali metal dopants can significantly improve the catalytic activity of NMO for the complete

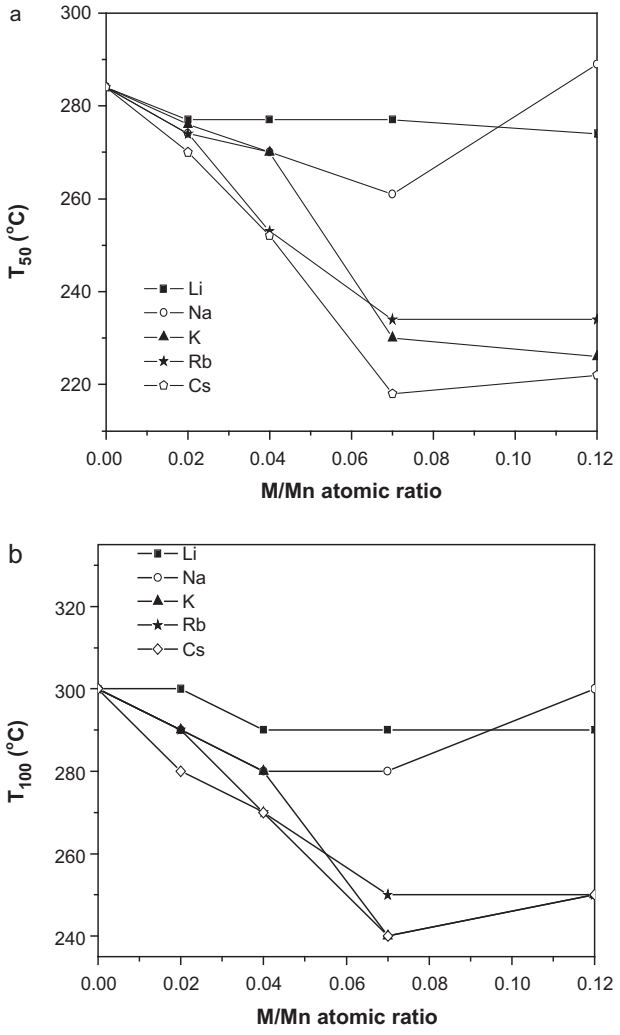

Fig. 2. Plots of T_{50} (a) and T_{100} (b) of the alkali metal-doped NMO catalyst as a function of M/Mn atomic ratio. Reaction conditions: *o*-xylene 550 ppm, 20% O_2/N_2 balance, total flow rate 50 mL min^{-1}, W/F = 0.60 g s mL^{-1}.

catalytic oxidation of *o*-xylene. Therefore, the effects of alkali metal on the catalytic performance and structural properties of NMO will be studied.

3.1.2. Optimal doping amounts of alkali metals

The atomic ratio of dopants ranged from x = 0.02 to 0.12. The T_{50} and T_{100} (the temperature needed to reach a CO_2 yield of 50% or 100%) of alkali metal doped NMO catalysts were used to optimize the atomic ratio of alkali metal to Mn (the calculated concentration of Mn in the NMO catalysts was 55% according to the EDS analysis). The reason for using the CO_2 yield to optimize the catalyst composition is that *o*-xylene can adsorb onto the surfaces of the catalysts, which may lead to over estimation of the catalytic oxidation activities [21]. Moreover, it should be taken into account that the use of complete *o*-xylene conversion may also lead to erroneous conclusions due to the formation of byproducts [21]. Therefore, the yield of CO_2 but not the complete conversion of *o*-xylene is used to evaluate the catalytic activity.

The results in Fig. 2 show that the optimal doping quantities of alkali metals were x = 0.12 for Li and approximately x = 0.07 for Na, K, Rb or Cs.

For the convenience of comparing the promotion effect of different alkali metals over a wide range of temperatures, catalytic activities of catalysts doped with optimal amounts of alkali metals

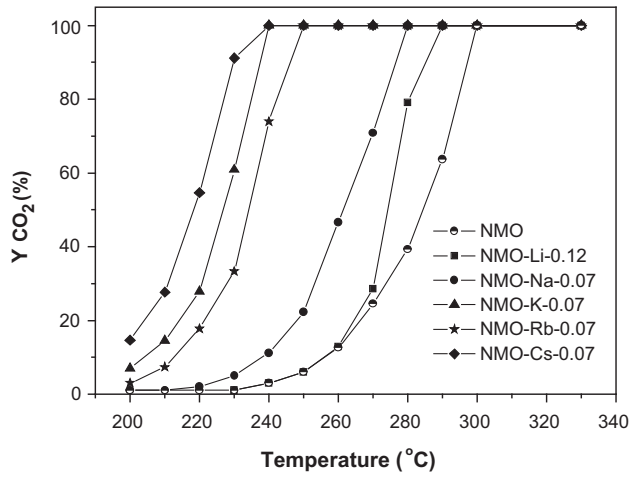

Fig. 3. Catalytic activities of NMO catalysts doped with optimal amounts of alkali metals for o-xylene complete catalytic oxidation. Reaction conditions: *o*-xylene 550 ppm, 20% O_2/N_2 balance, total flow rate 50 mL min^{-1}, W/F = 0.60 g s mL^{-1}.

are shown in Fig. 3.

It can be seen that the alkali metals investigated improve the activity of NMO catalyst for the complete catalytic oxidation of *o*-xylene in the following sequence: Li < Na < Rb < K, Cs. Although alkali metal oxides were reported to be good promoters on cobalt–cerium composite oxide catalysts for N_2O decomposition [18], the promoter effect of alkali metal compounds on NMOs for the complete catalytic oxidation of VOCs has not been reported. The present study suggests that small amounts of alkali metal oxides can remarkably improve the catalytic activity of NMO catalysts. In general, across the group, as the atomic radius increases, the promotion effect increases. It is irrefutable that the promotion effects of Li and Na are much lower than that of Rb, K and Cs. As for Rb, K and Cs, it was found that the T_{100} of the NMO-K-0.07 and the NMO-Cs-0.07 catalysts was 240 °C, which is 10 °C lower than that of the NMO-Rb-0.07 catalyst. When the temperature was lower than 240 °C, the activity sequence changed to: Rb < K < Cs. Although the promotion effect did not strictly follow the descending periodic order of the alkali metal group Li, Na, K, Rb, and Cs, the sequence of catalytic activity Li < Na < Rb < K, Cs suggests that the promotion effect relate to the period of the element. Therefore, we deduce that the alkali metals promote the activity of the NMO by an electronic effect. To obtain evidence to support this assumption, extensive characterization was carried out on K-doped NMO catalysts.

3.2. Characterization of NMO and NMO-K-x catalysts

3.2.1. EDS results of NMO

The chemical composition of the natural manganese ore were analyzed using an energy dispersive spectrometer (EDS). The EDS result (Fig. 4) shows that the Mn concentration in the NMO catalyst is up to 55%. The remainder was composed of 21.76% Si, 17.5% Fe, and a minor quantity of K, Al, Ca, and Ti. As we all know, Si and its oxide are normally considered inactive for catalytic oxidation. In order to reveal whether Fe and Fe_xO_y or other Fe-based oxides are active in the NMO, we synthesized some manganese oxides: MnO_2, Mn_2O_3, and Mn_3O_4, and compared their activities with NMO under the same conditions. It was found that the prepared manganese oxides (T_{100} of the as-prepared MnO_2, Mn_2O_3, and Mn_3O_4 were 250 °C, 270 °C, and 280 °C, respectively) were more active than NMO, which suggests that other components in NMO, such as Fe and Fe_xO_y in NMO were inactive in our experiments.

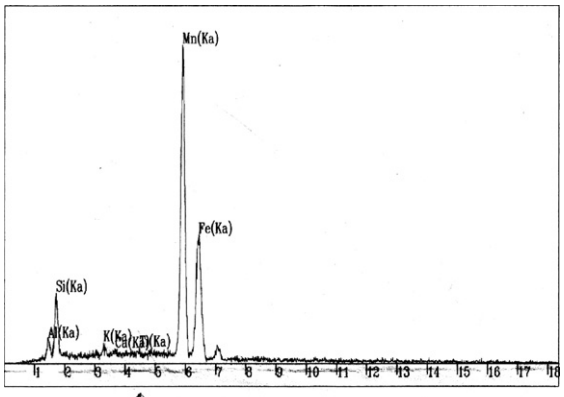

Element	Line	Weight %	Atomic %	Rel. Error	ZAF	Z	A	F
Mn	(Ka)	55.10	44.66	1.70	1.105	1.041	1.062	1.000
Fe	(Ka)	17.50	13.95	2.59	1.054	1.020	1.033	1.000
Al	(Ka)	1.37	2.26	7.79	5.254	0.944	5.652	0.984
Si	(Ka)	21.76	34.50	4.30	3.536	0.918	3.873	0.995
K	(Ka)	1.99	2.27	8.71	1.491	0.955	1.594	0.979
Ca	(Ka)	1.30	1.45	8.74	1.317	0.935	1.447	0.973
Ti	(Ka)	0.98	0.91	10.06	1.180	1.023	1.219	0.946

Fig. 4. EDS results of NMO catalysts.

3.2.2. XRD and BET results of NMO and NMO-K-x

The X-ray diffraction (XRD) measurement was conducted to determine the bulk crystalline phase of the NMO and NMO-K-*x* catalysts, see Fig. 5. The NMO and NMO-K-*x* catalysts showed similar XRD patterns, revealing an amorphous or microcrystalline structure with a weak peak at $2\theta = 26.6^{\circ}$. The weak peaks were attributed to Fe_2O_3 [22]. According to the EDS analysis of NMO, the amorphous or microcrystalline structure may be due to a complex of MnO_x and the other metal oxides. As for the NMO-K-*x* catalysts, there are no evidence from the diffraction patterns of K_2O formation when the Mn/K atomic ratio was varied. The absence of the K_2O diffraction on the NMO-K-*x* catalysts suggests that the alkali metal may be highly dispersed on the surface of the NMO catalyst or amorphous. Although the presence of alkali metals promotes the catalytic activity of the NMO, it hardly affects the crystal phases of the catalyst.

In order to investigate the influence of the addition of alkali metals on the surface properties of NMO, the BET surface areas of NMO-Li-0.12 (the catalyst with worst catalytic activity in our study), NMO-K-0.07 (the catalyst with best catalytic activity in our study) and NMO were measured. The BET surface area of NMO-Li-0.12 ($50\,m^2\,g^{-1}$) and NMO-K-0.07 ($54\,m^2\,g^{-1}$) were similar to that of NMO ($63\,m^2\,g^{-1}$). Therefore, it can be concluded that the addition of alkali metal promoters did not have a significant effect on the specific surface areas of the catalysts. Namely, the doping alkali metals are not structural promoters.

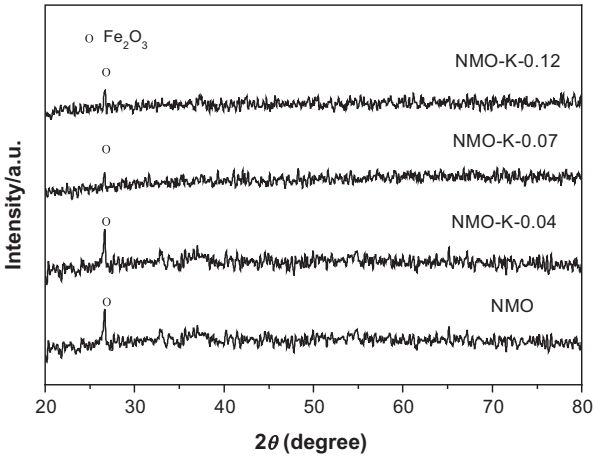

Fig. 5. XRD patterns of NMO-K-*x* catalysts.

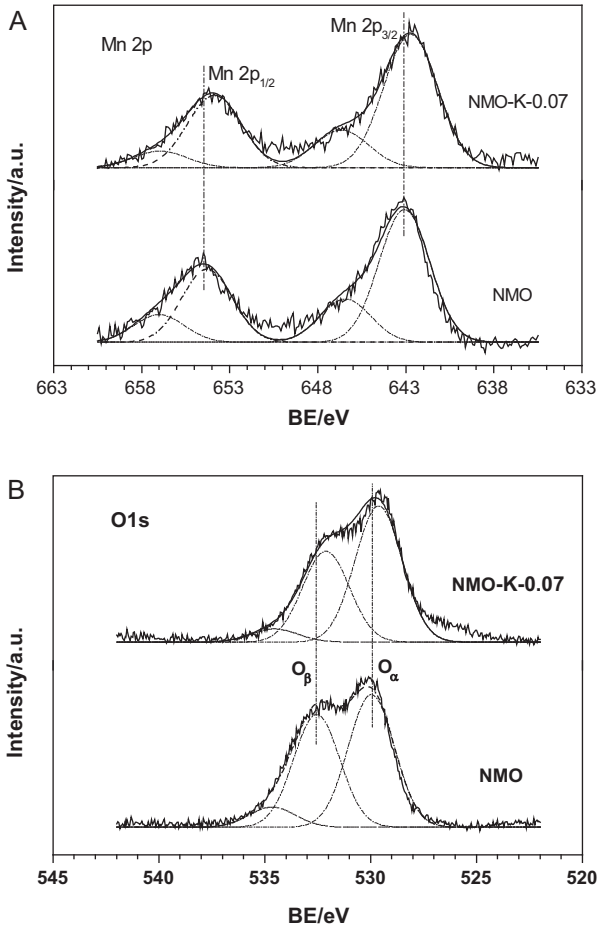

Fig. 6. XPS spectra of Mn 2p(A) and O 1s (B) of the NMO-K-0.07 and NMO catalysts.

3.2.3. XPS results of NMO and NMO-K-0.07

The NMO and NMO-K-0.07 catalysts were also examined via XPS to determine the oxidation state and the influence of alkali metals on the valence states of the main phase of Mn. Fig. 6A shows the XPS spectra of Mn 2p of the NMO and NMO-K-0.07 catalysts (the satellite peaks at 646.0–647.0 eV, which likely originated from the charge transfer between the outer electron shell of the ligand, and the unfilled 3d shell of Mn during the creation of the core–hole in the photoelectron process were also considered [23]). For the NMO catalyst, the binding energies (BE) of the Mn $2p_{3/2}$ and Mn $2p_{1/2}$ peaks were 642.6 and 654.1 eV, respectively. The $2p_{3/2}$–$2p_{1/2}$ spin orbit splitting (ΔE) of NMO was 11.5 eV. As for the NMO-K-0.07 catalyst, the BE of the Mn $2p_{3/2}$ and Mn $2p_{1/2}$ peaks both shifted to a lower value compared to NMO. A similar negative BE shift of Co $2p_{3/2}$ in K-doped Co_3O_4 was also reported by He and co-workers [18]. The new Mn $2p_{3/2}$ and Mn $2p_{1/2}$ BE were 642.2 and 653.7 eV, respectively, and the ΔE remained at 11.5 eV. According to the literature, ΔE is very useful for elucidating the oxidation state of Co_3O_4 [18]. As long as the $2p_{3/2}$–$2p_{1/2}$ spin orbit splitting (ΔE) was 15.1 eV, the existence of Co_3O_4 could be inferred despite the change in the Co BE due to various chemical environments [18]. The XPS spectra of Mn $2p_{3/2}$ in NMO and NMO-K-0.07 are consistent with the reported range of 642.1–643 eV for MnO_2 in the literature [13]. Therefore, it was deduced that MnO_2 is the main active phase in the NMO and NMO-K-0.07 catalysts. The addition of K to the

Table 1
XPS results of the NMO and NMO-K-0.07 catalysts.

Sample	BE(eV)			$O_\alpha/(O_\alpha+O_\beta)$ (100%)
	Mn^{4+}	O_α	O_β	
NMO-K-0.07	642.2	529.6	532.1	56.7
NMO	642.6	530.0	532.5	50.0

catalysts did not change the valance state of manganese (ΔE remained at 11.5 eV); however, the chemical environment of Mn ion in the NMO-K-0.07 catalyst was most likely affected. The electronic effect of K was believed to be a major reason for the change of the chemical environments of the Mn ion in the NMO-K-0.07 catalyst, and a major contributor to its high activity.

The XPS spectra for O1s in the NMO and NMO-K-0.07 catalysts are shown in Fig. 6B. Three types of oxygen species were identified through deconvolution of the spectra. The BE at 529–530 eV was ascribed to the lattice oxygen (denoted as O_α) and the BE at 531–532 eV was ascribed to defective oxides or surface oxygen ions with low coordination (denoted as O_β) [24]. The peak at the higher binding energy peak (above 533 eV) corresponds to adsorbed molecular water [25]. Table 1 shows that the O_α contents were 56.7% and 50.0% for the NMO-K-0.07 and NMO catalysts, respectively. Obviously, the NMO-K-0.07 catalyst possessed more lattice oxygen species than the NMO catalyst. Based on the fact that NMO-K-0.07 showed much higher catalytic activity for complete catalytic oxidation of *o*-xylene, we deduced that O_α, not O_β, is the main active oxygen species and is responsible for the high catalytic activity of NMO-K-0.07 in the complete oxidation of *o*-xylene.

3.2.4. H_2-TPR

H_2-TPR experiments of NMO, NMO-K-0.04, NMO-K-0.07 and NMO-K-0.12 catalysts were carried out to examine the influence of the alkali metals on the reduction behavior of the NMO catalyst. High contents of Si and Fe were detected in NMO by EDS. Si and its oxide are normally considered to be inactive for catalytic oxidation. Considering NMO itself exhibited lower activity than various pure Mn_xO_y (results not shown) for the complete catalytic oxidation of *o*-xylene, Fe and/or Fe_xO_y were also assumed to be inactive. Although the reduction peaks of Fe and/or Fe_xO_y are similar to manganese oxides, the exact estimation of the phase change of NMO was difficult because NMO was composed of various metal oxides. We omitted the reduction of Fe_xO_y and assumed that these reduction peaks were attributed to manganese oxides. The TPR profiles are shown in Fig. 7. There were two reduction peaks in the profiles. The peak centered at ca. 365–375 °C (P_{H2}-I) is attributed to the reduction of MnO_2 to Mn_2O_3. P_{H2}-II in the region of 445–467 °C is due to the reduction of Mn_2O_3 to MnO [13,25].

As can be seen in Fig. 7, the reduction behavior of the catalyst is greatly influenced by the addition of K. The area of the H_2 consumption peaks increases in the following order: NMO < NMO-K-0.04 < NMO-K-0.12 < NMO-K-0.07. This sequence is in the same order as that of the catalytic activity. Moreover, with increasing K content, the P_{H2}-I peak remained relatively in the same position, while P_{H2}-II peaks shift slightly to lower temperatures, for example, from 467 °C for NMO to 445 °C for NMO-K-0.12. The TPR results suggest that the presence of alkali metals increase the reducibility of Mn^{4+} to Mn^{3+} and Mn^{3+} to Mn^{2+}. According to the XPS results, the addition of K to NMO affected the chemical environment of the Mn ion and increased the content of O_α. It was reasoned that the Mn–O bond strength might be weakened by the addition of K, which further promoted the mobility and availability of lattice oxygen species in NMO. Thus, the reduction behavior of NMO was

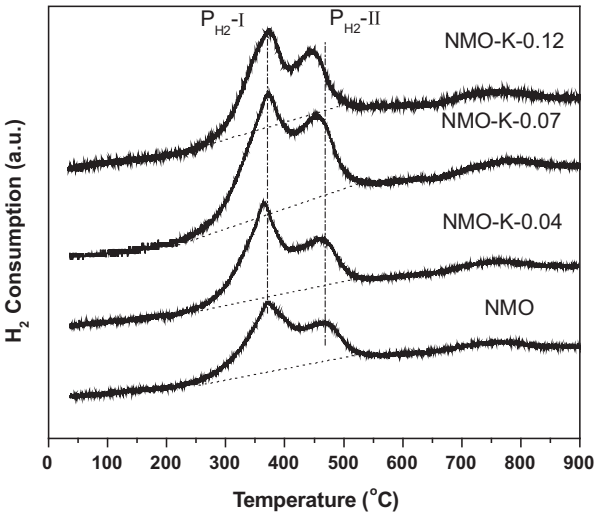

Fig. 7. H_2-TPR profiles of NMO-K-*x*.

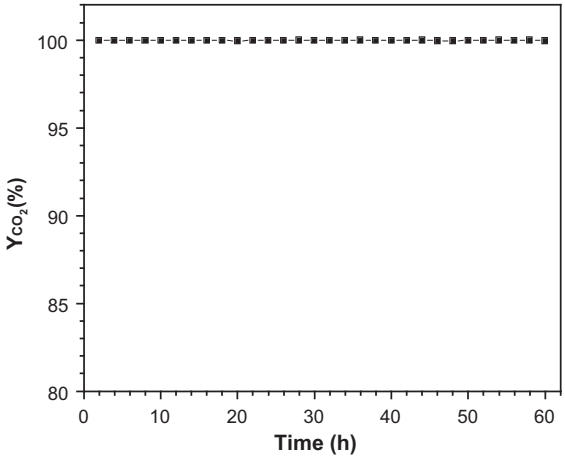

Fig. 8. CO_2 yield versus on stream time over the NMO-K-0.07 catalyst. Reaction conditions: *o*-xylene 550 ppm, 20% O_2/N_2 balance, total flow rate 50 mL min^{-1}, W/F = 0.60 g s mL^{-1}.

enhanced and its catalytic activity was improved. The TPR results for NMO-K-0.07 catalyst are consistent with that of the Mn 2p and O1s XPS analysis.

On the basis of the H_2-TPR and XPS results, it was deduced that trace additions of alkali metals affect the chemical environment of the Mn ion and weaken the Mn–O bond strength, which further promoted oxygen mobility of NMO. These effects caused by the addition of alkali metals are responsible for the activity enhancement of NMO.

3.3. Stability test for NMO-K-0.07 catalyst

In the isothermal combustion of *o*-xylene at 240 °C for 60 h over NMO-K-0.07 the CO_2 yield remained at 100% for the duration of the test. This result indicates that NMO-K-0.07 is relatively stable under these working conditions (Fig. 8).

4. Conclusions

This study found that the addition of alkali metals to NMO catalyst caused a remarkable increase in catalytic activity for the complete oxidation of *o*-xylene. The promotion effect of these promoters followed the order Li < Na < Rb < K, Cs. At 240 °C, 100% CO_2

yield were achieved over NMO-K(Cs)-0.07 catalysts, which was 60 °C lower than the temperature required for NMO. According to the results of the characterization, MnO_2, which has a microcrystalline structure in NMO was the main active phase, and the addition of the alkali metals did not have a great influence on the crystal structure and specific surface area of the NMO catalyst. However, the chemical environments of Mn ions appeared to be affected by the doped alkali metals. Moreover, the addition of alkali metals not only improves the reducibility of Mn ions but also increase the lattice oxygen content and its mobility. Lattice oxygen is the main active oxygen species and is responsible for the high catalytic activity of alkali metal doped catalysts in the complete oxidation of *o*-xylene. The alkali metal doped NMOs are high potential catalysts for the catalytic oxidation of VOCs.

Acknowledgements

The authors would like to thank Prof. Hong He for stimulating suggestion and experimental assistance from his research group in RCEES, Chinese Academy of Sciences.

This work is supported by the National Natural Science Foundation of china (no. 20977024), the Natural Science Foundation of Hebei Province (no. B2009000258), the Natural Science Foundation of Hebei Education Department (no. 2008128) and Doctoral Foundation of Hebei Normal University (no. L2005B16, L2006Y04).

References

[1] C. Lahousse, A. Bernier, P. Grange, B. Delomn, P. Papaefthimiou, T. Ioannides, X. Verykios, J. Catal. 178 (1998) 214.
[2] H.L. Tidahy, S. Siffert, F. Wyrwalski, J.F. Lamonier, A. AboukĬs, Catal. Today 119 (2007) 317.
[3] R.S.G. Ferreira, P.G.P. de Oliveira, F.B. Noronha, Appl. Catal. B 50 (2004) 243.
[4] H. Kim, T. Kim, H. Koh, S. Lee, B. Min, Appl. Catal. A 280 (2005) 125.
[5] J. Li, X. Xu, Z. Jiang, Z. Hao, C. Hu, Environ. Sci. Technol. 39 (2005) 1319.
[6] T. Garcia, B. Solsona, D. Cazorla-Amoroïs, A. Linares-Solano, S.H. Taylor, Appl. Catal. B 62 (2006) 66.
[7] S.C. Kim, J. Hazard. Mater. B 91 (2002) 285.
[8] W.B. Li, W.B. Chu, M. Zhuang, J. Hua, Catal. Today 93-95 (2004) 205.
[9] W.B. Li, J.X. Wang, H. Gong, Catal. Today 148 (2009) 81.
[10] H. Einaga, S. Futamura, J. Catal. 227 (2004) 304.
[11] L. Lamaita, M.A. Peluso, J.E. Sambeth, H.J. Thomas, Appl. Catal. B 61 (2005) 114.
[12] C. Cellier, V. Ruaux, P. Grange, E.M. Gaigneaux, Catal. Today 117 (2006) 350.
[13] D. Delimaris, T. Ioannides, Appl. Catal. B 84 (2008) 303.
[14] Y.S. Wu, Y.X. Zhang, M. Liu, Z.C. Ma, Catal. Today 153 (2010) 170.
[15] M. Kang, E.D. Park, J.M. Kim, J.E. Yie, Appl. Catal. A 327 (2007) 261.
[16] M.R. Morales, B.P. Barbero, L.E. Cadús, Appl. Catal. B 67 (2006) 229.
[17] J.Y. Lee, S.B. Kim, S.C. Hong, Chemosphere 50 (2003) 1115.
[18] L. Xue, H. He, C. Liu, C.B. Zhang, B. Zhang, Environ. Sci. Technol. 43 (2009) 890.
[19] L.M. Gandía, A. Gil, S.A. Korili, Appl. Catal. B 33 (2001) 1.
[20] K. Jirátová, J. Mikulová, J. Klempa, T. Grygar, Z. Bastl, F. Kovanda, Appl. Catal. A 361 (2009) 106.
[21] S.Y. Huang, C.B. Zhang, H. He, Catal. Today 139 (2008) 115.
[22] J. Li, Y. Zhan, X. Lin, Acta Phys. Chim. Sin. 246 (2008) 932.
[23] M. Ferrandon, J. Carnö, S. Järas, E. Björnbom, Appl. Catal. A 180 (1999) 141.
[24] X. Tang, Y. Li, X. Huang, Y. Xu, H. Zhu, J. Wang, W. Shen, Appl. Catal. B 62 (2006) 265.
[25] T.F. Tian, M.C. Zhan, W.D. Wang, C.S. Chen, Catal. Commun. 10 (2009) 513.